JACS
JOURNAL OF THE AMERICAN CHEMICAL SOCIETY
pubs.acs.org/JACS
Article

Peptidomimetic Wet-Adhesive PEGtides with Synergistic and Multimodal Hydrogen Bonding

Minseong Kim,[‖] Jinwoo Park,[‖] Kyung Min Lee,[‖] Eeseul Shin, Suebin Park, Joonhee Lee, Chanoong Lim, Sang Kyu Kwak,* Dong Woog Lee,* and Byeong-Su Kim*

Cite This: *J. Am. Chem. Soc.* 2022, 144, 6261−6269

ABSTRACT: The remarkable underwater adhesion of mussel foot proteins has long been an inspiration in the design of peptidomimetic materials. Although the synergistic wet adhesion of catechol and lysine has been recently highlighted, the critical role of the polymeric backbone has remained largely underexplored. Here, we present a peptidomimetic approach using poly(ethylene glycol) (PEG) as a platform to evaluate the synergistic compositional relation between the key amino acid residues (*i.e.*, DOPA and lysine), as well as the role of the polyether backbone in interfacial adhesive interactions. A series of PEG-based peptides (PEGtides) were synthesized using functional epoxide monomers corresponding to catechol and lysine *via* anionic ring-opening polymerization. Using a surface force apparatus, highly synergistic surface interactions among these PEGtides with respect to the relative compositional ratio were revealed. Furthermore, the critical role of the catechol−amine synergy and diverse hydrogen bonding within the PEGtides in the superior adhesive interactions was verified by molecular dynamics simulations. Our study sheds light on the design of peptidomimetic polymers with reduced complexity within the framework of a polyether backbone.

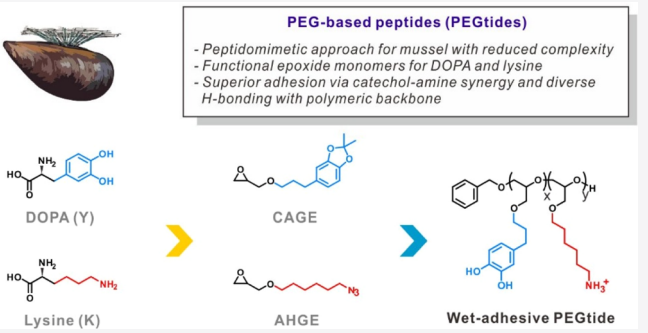

INTRODUCTION

Recent advances in synthetic chemistry have opened pathways to generate relatively simple peptide-like structures and functions using nonbiological synthetic polymers.[1−4] While it is still challenging for a single polymer system to simultaneously achieve a long primary chain, stable secondary structure, and sequence diversity, the unusual stability and versatility of peptidomimetic polymers have made them ideal candidates for developing unique functional materials from relatively inexpensive building blocks with diverse characteristics.[3] Representative examples include synthetic polypeptides, peptoids, polyacrylates, and poly(methyl methacrylate)s bearing constitutional amino acid residues found in nature.[5−9] However, most polymeric mimics comprise an all-carbon backbone, which makes them structurally rigid and intrinsically insoluble in aqueous solutions. These limitations often are challenging for creating systems with the full potential to mimic natural polypeptides.

The outstanding adhesive performance of the mussel foot protein (*mfp*) in the byssal threads has long been a source of inspiration for designing novel functional materials.[10] In particular, the discovery of 3,4-dihydroxylphenylalanine (DOPA)—a major catecholic amino acid responsible for the versatile surface adhesion—has led to a surge of mussel-inspired adhesives and coatings.[11−20] While DOPA has been in the spotlight for decades, other amino acid residues present in *mfp*, particularly cationic amino acid residues such as lysine, have recently attracted growing attention because of their synergistic interplay that leads to enhanced wet adhesion on account of diverse intermolecular interactions including metal coordination,[18,21] electrostatic interactions,[22] cation−π interactions,[17,23,24] and covalent crosslinking.[18,19,25−27] As a representative example, Waite and co-workers first showed that neighboring catechol and lysine groups can have synergistic interactions, in which the cationic lysine displaces the hydrated salts to produce vacant binding sites for the adhesion of catechol *via* small molecular analogues of siderophore.[28,29] Furthermore, this synergistic effect between catechol and amine have been explored in the context of polymers. For example, Ahn and co-workers revealed the importance of the balance between electrostatic and hydrophobic interactions to enhance wet adhesion *via* coacervation.[27] Recently, Messersmith and co-workers demonstrated that the coupling of catechol and amines in the same monomer side chain affords optimal cooperative effects in improving the

Received: November 9, 2021
Published: March 17, 2022

https://doi.org/10.1021/jacs.1c11737
J. Am. Chem. Soc. 2022, 144, 6261−6269

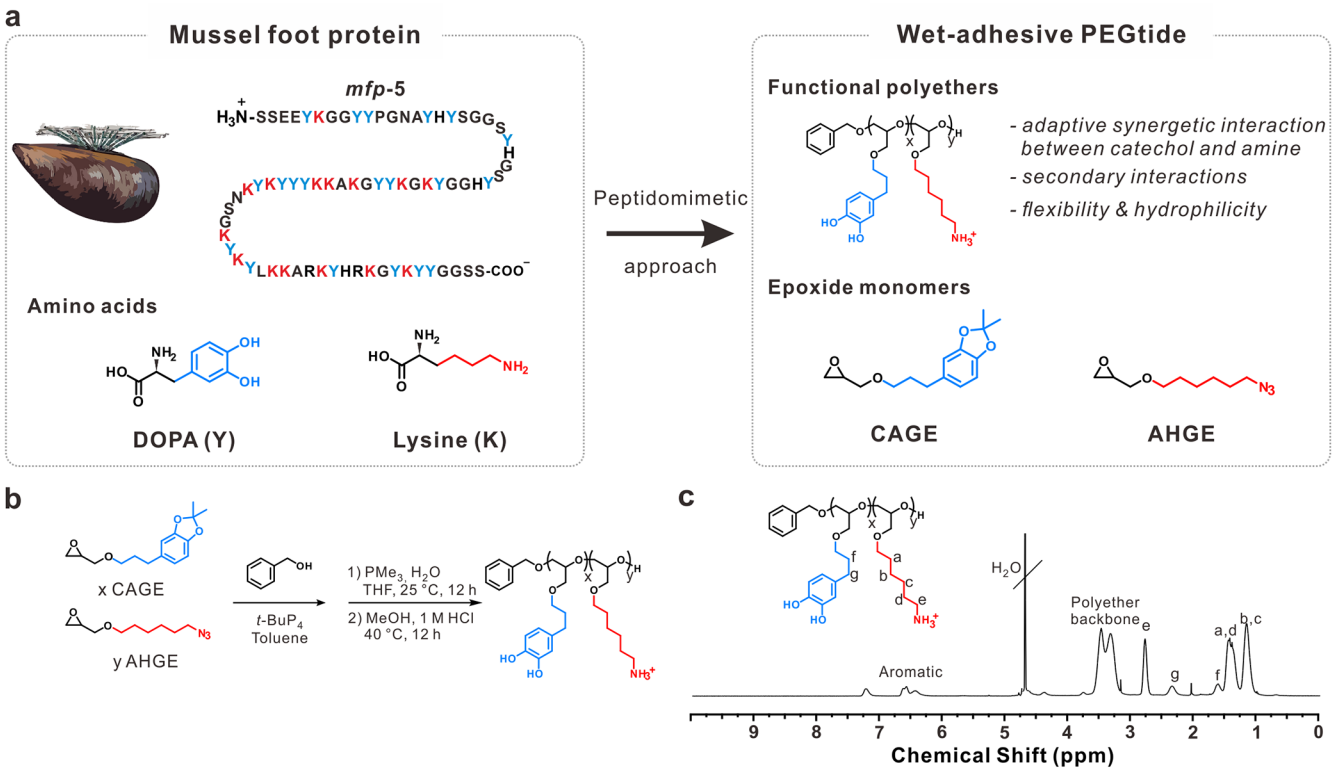

Figure 1. Synthesis of PEGtides. (a) Schematic illustration of peptidomimetic PEGtides bearing catechol and amine moieties, based on the primary sequence of *mfp*-5. (b) Synthetic procedures and (c) representative ^{1}H NMR spectrum of the PEGtide (AC1 in Table 1).

macroscopic wet/dry adhesion performance in a system with only 2.85% of the functional methacrylate monomer.[30] These studies highlighted the cation−π interactions between catechol and amine, as well as the bidentate hydrogen bonding (H-bonding) between catechols.

Despite the discovery of synergistic interplay of catechol and amine, the critical role of the polymeric backbone with respect to the side chains has been relatively underexplored.[31] Moreover, considering that the biological activity of peptides is significantly affected by their secondary structure owing to the strong and regular intermolecular interactions, such as H-bonding between the polypeptide backbone and the side chains, an alternative peptidomimetic approach affording additional intermolecular interactions between the backbone and side chains is highly desirable for maximizing the catechol−amine synergy.

Herein, we propose a mussel-inspired peptidomimetic approach by employing poly(ethylene glycol) (PEG) as a platform to investigate the synergistic compositional relationship of the key amino acid residues (*i.e.*, catechol and lysine), as well as the role of the polymeric backbone in interfacial adhesive interactions. The polyether backbone was selected to offer flexibility, solubility, high biocompatibility, and non-immunogenicity.

Specifically, a series of PEG-based peptides (PEGtides) were synthesized using well-defined functional epoxide monomers—catechol acetonide glycidyl ether (CAGE) and azidohexyl glycidyl ether (AHGE)—corresponding to DOPA and lysine, respectively, *via* anionic ring-opening polymerization (Figure 1a). Subsequent deprotection and reduction of the polymers yielded the functional PEGtides with controlled side-chain functionalities (*i.e.*, the fraction of catechol ranging within 0−100%) and molecular weights (4000−16 000 g/mol). The surface adhesive properties of these PEGtides were carefully examined using a surface force apparatus (SFA) under various conditions. The SFA analysis revealed an optimum compositional ratio between the catechol and amine for maximum adhesion energy (52.52 mJ/m^2). Furthermore, the adhesive interaction of PEGtides was theoretically elucidated using molecular dynamics (MD) simulations to determine the contributions of the diverse intermolecular interactions therein [*e.g.*, cation−π, aromatic−aromatic (Ar−Ar), and H-bonding] and polyether backbone on the highly adhesive properties of synthesized PEGtides.

RESULTS AND DISCUSSION

Preparation of PEGtides. To explore the synergistic adhesive characteristics of DOPA and lysine, their corresponding monomers (CAGE and AHGE) based on a functional epoxide system were designed, synthesized by a simple substitution reaction, and subjected to fractional distillation to achieve high purity (>99%) monomers (Figures S1−S8).[32,33] Due to the harsh reaction conditions during the anionic ring-opening polymerization, CAGE and AHGE were protected with acetonide and azide groups, respectively. A metal-free organic phosphazene, *t*-BuP$_4$, was used as a base owing to its high basicity and, more importantly, its facile polymerization at room temperature without side reactions. To eliminate the effects of molecular weight, such as wetting, viscosity, and chain entanglement, the degree of polymerization (DP) was set to 20.[22]

Using benzyl alcohol as an initiator, polymerization was performed with different fractions of CAGE and AHGE (*i.e.*, CAGE fraction was varied from 0 to 100%) in toluene at room temperature (Table 1 and Figure 1b). The conversion of

https://doi.org/10.1021/jacs.1c11737
J. Am. Chem. Soc. 2022, 144, 6261−6269

Table 1. Characterizations of the PEGtides Prepared in This Study

			pre-PEGtide[a]			PEGtide[c]
entry	composition (NMR)	f_{CAGE} (%)	$M_{n,NMR}$ (g/mol)	$M_{n,GPC}$[b] (g/mol)	$Đ$[b]	$M_{n,NMR}$ (g/mol)
AC0	$PAHGE_{21}$	0	4200	5700	1.06	3680
AC1	$P(AHGE_{15}$-*co*-$CAGE_5)$	25	4520	4190	1.17	3920
AC2	$P(AHGE_{10}$-*co*-$CAGE_{11})$	52	5000	4100	1.07	4600
AC3	$P(AHGE_5$-*co*-$CAGE_{17})$	77	5480	5160	1.11	4670
AC4	$PCAGE_{21}$	100	5820	5290	1.28	4980

[a]Protected P(AHGE-*co*-CAGE)s. [b]Determined by GPC in THF with PMMA calibration. [c]Deprotected PEGtides.

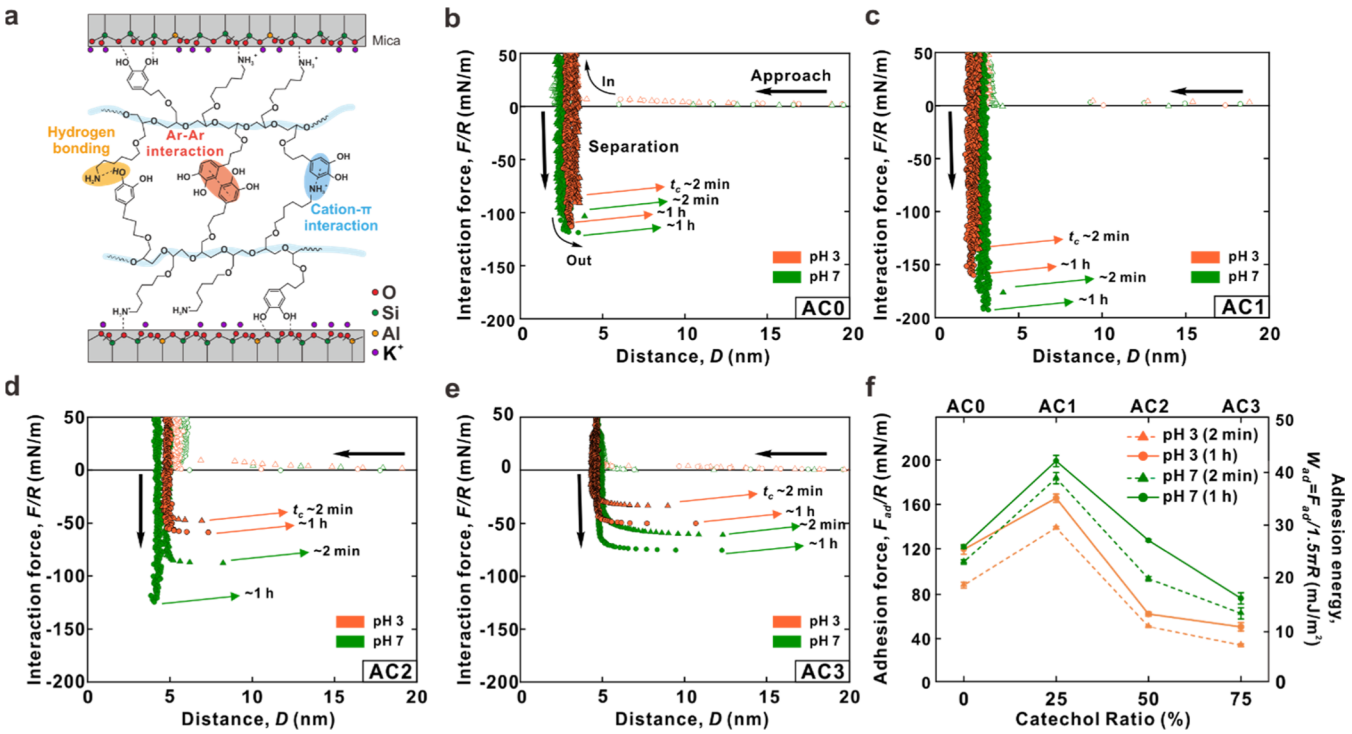

Figure 2. Adhesion energy measurement of PEGtides with mechanism analysis. (a) Schematic representation of the symmetric SFA analysis (polymer *vs* polymer) with the possible types of interactions. (b–e) Representative symmetric force–distance curves of (b) AC0, (c) AC1, (d) AC2, and (e) AC3 PEGtides. (f) Plots of (left) the measured adhesion force and (right) adhesion energy of the PEGtides at different pH and contact times (see the Materials and Methods section for details).

monomers was monitored *via* ^{1}H NMR spectroscopy by observing the decrease in the methine and methylene signals of the epoxide monomers at 3.15, 2.80, and 2.60 ppm (Figures S2, S6, and S9), indicating the successful polymerization of $P(AHGE$-*co*-$CAGE)_n$ (*i.e.*, the pre-PEGtides prior to deprotection) with over 99% conversion in 18 h.

Furthermore, the gel permeation chromatography (GPC) results of the copolymers exhibited a unimodal distribution and narrow dispersity ($Đ$ = 1.06–1.28) (Figures S9 and S10; Table 1). Moreover, the reactivity ratio between the pair of monomers was examined *via in situ* ^{13}C NMR spectroscopy using the inverse-gated decoupling method. A nonterminal model was used to obtain the reactivity ratios of AHGE and CAGE: r_{AHGE} = 1.09 ± 0.01 and r_{CAGE} = 0.91 ± 0.01, respectively. This revealed the ideal copolymerization that yielded the statistical microstructures ($r_{AHGE} \times r_{CAGE}$ = 0.99 ± 0.01) in the resulting copolyethers (Figure S11).[34]

After their successful synthesis, the P(AHGE-*co*-CAGE) copolymers (*i.e.*, pre-PEGtides) were further treated with PMe_3 for Staudinger reduction of the azide groups in AHGE, followed by treatment with 1.0 M HCl to deprotect the acetonide groups in CAGE to yield the desired PEGtides (Figures 1c and S9; the AC series in Table 1). Complete removal of the protecting groups was confirmed in ^{1}H NMR spectra by the disappearance of the acetonide group at 1.58 ppm and the shift of the methine group neighboring the azide group from 3.08 to 2.30 ppm. In addition, reduction of the azide group was confirmed *via* FT-IR, with the disappearance of peaks corresponding to the azide pendant at 2088 cm^{-1} (Figure S12).

Interaction Force Analysis Using SFA and MD Simulations. All the synthesized PEGtides with well-defined structures were coated onto mica substrates, and surface interaction forces of the PEGtides were evaluated using an SFA. The SFA analysis has been widely adopted to measure the absolute distances (D) and interaction forces (F) between two macroscopic surfaces with remarkable resolutions of 0.1 nm and 10 nN, respectively, mostly in aqueous media. The adhesion force (F_{ad}) can be obtained from the magnitude of the minimum interaction forces (typically before the jump-out during separation) and converted to the adhesion energy (W_{ad}) using the Johnson–Kendall–Roberts theory of adhesive

https://doi.org/10.1021/jacs.1c11737
J. Am. Chem. Soc. 2022, 144, 6261–6269

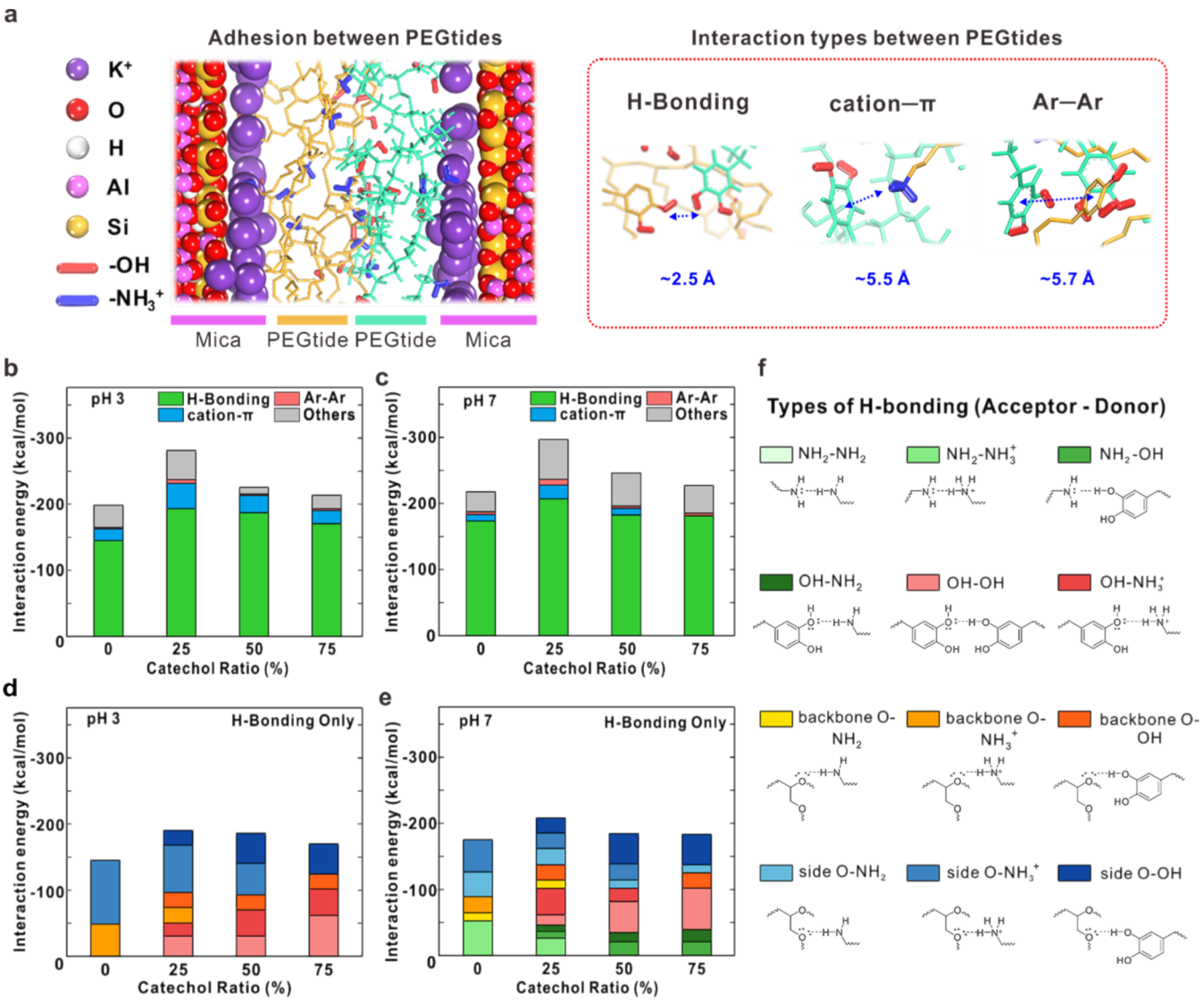

Figure 3. (a) Schematics of the MD simulation system and the main types of molecular interactions considered. (b−e) Calculated interaction energy between PEGtides at the interface at (b) pH 3 and (c) pH 7, and the types of H-bonding at (d) pH 3 and (e) pH 7. (f) Twelve different types of H-bonding considered in the calculations for j and k.

surfaces ($W_{ad} = F_{ad}/1.5\pi R$, see the Materials and Methods section for details).[35]

Figure 2a shows the schematic of the SFA experiment for measuring the interaction forces between two PEGtide-coated mica surfaces, along with the force−distance profiles obtained at different catechol contents (PEGtides AC0−AC3), contact times (t_c = 2 min and 1 h), and pH (3 and 7) (Figure 2b−e). Note that the AC4 sample was excluded due to its limited aqueous solubility. Moreover, there was no phase separation or coacervate formation in all SFA measurement conditions.

When two polymer-coated surfaces were brought near each other, they jumped into contact with a hard-wall distance of 3.0 ± 0.4 (AC0), 2.7 ± 0.4 (AC1), 4.4 ± 0.4 (AC2), and 4.7 ± 0.2 nm (AC3). Here, half of the hard-wall distance corresponds to the polymer film thickness. The hard-wall thickness increased as the proportion of catechol monomer increased. When the two surfaces were separated, the corresponding force−distance curves displayed an abrupt jump-out behavior, indicating strong adhesion (F_{ad}) between the PEGtide films. In all the experiments, W_{ad} generally increased with t_c because the polymer chains required a lab-scale time to attain interfacial equilibration, as commonly observed in systems that undergo molecular rearrangement upon contact for maximum binding of the adhesion sites.[36−38] In this study, two different pH conditions were used to modulate the degree of protonation of the amine groups because protonated amines serve as cationic sources for cation−π and electrostatic interactions during the adhesion among PEGtides and as H-bonding donors. Our SFA results showed that a higher W_{ad} was generally obtained at pH 7, when the fraction of ammonium groups in the PEGtides was smaller than that of the free amines. Notably, no pH-dependent chemical or structural changes were observed in our system at pH 7 (Figures S13 and S14), unlike previous studies in which natural *mfp*-5 and *mfp*-3 experienced oxidation of DOPA at pH 5.5, leading to significantly lower adhesion compared to that at pH 3.[16,19] In addition, there was no remarkable changes in the hard-wall thickness upon pH changes, suggesting the absence of secondary structures in the PEGtide system.

https://doi.org/10.1021/jacs.1c11737
J. Am. Chem. Soc. 2022, 144, 6261−6269

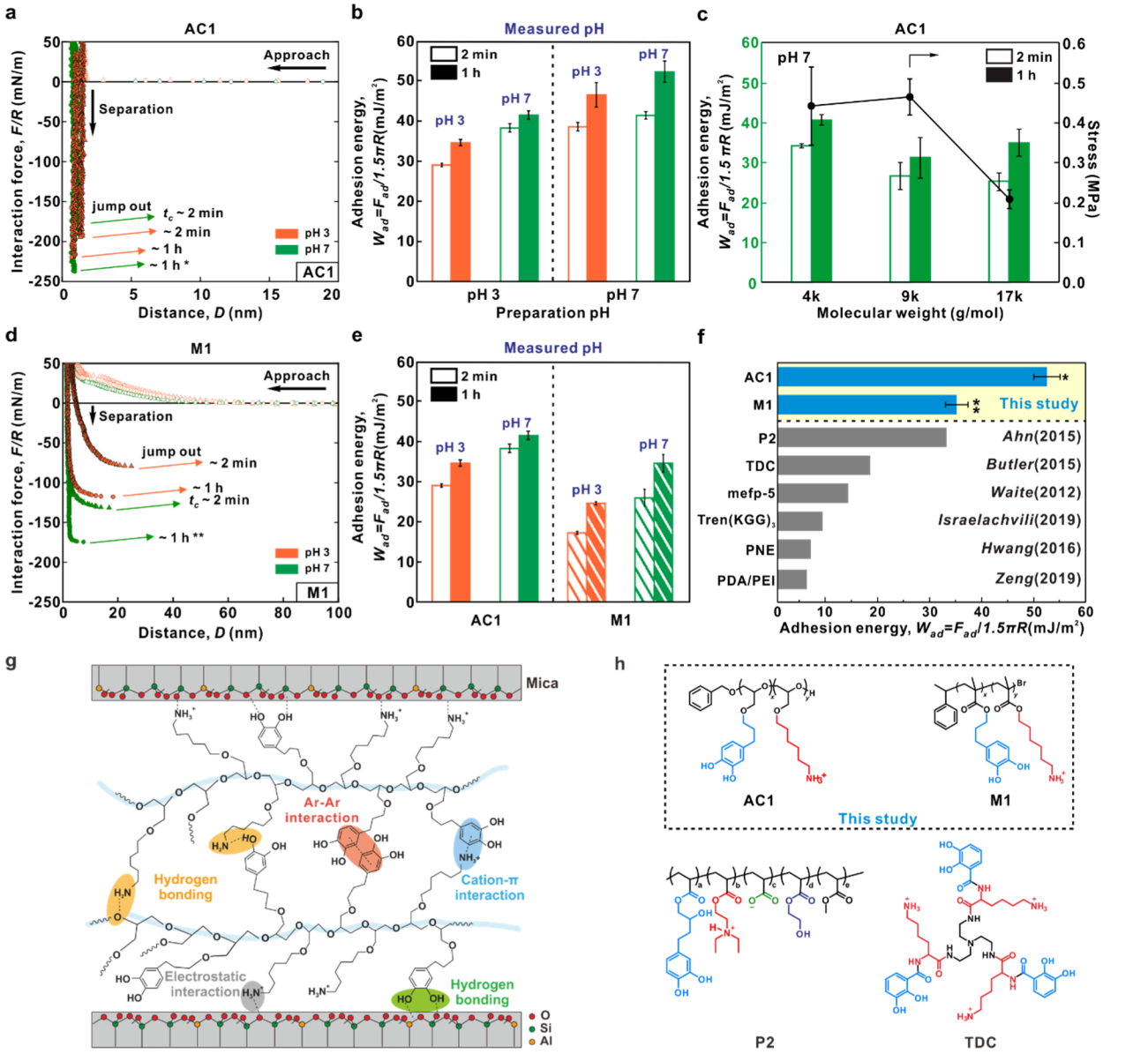

Figure 4. Optimizing surface interaction forces of the PEGtides through various controls. (a) Representative symmetric force−distance curves of AC1 prepared at pH 7 and measured at pH 3 and 7. (b) Adhesive energy of AC1 under different preparation and measurement pH conditions. (c) Plots of (left) the adhesive energy and (right) shear stress of AC1 polymers with different molecular weights. (d) Representative symmetric force−distance curves of M1. (e) Comparison of the adhesion energy of AC1 and M1 with different t_c and measurement pH. (f) Bar chart comparing the adhesion energies of AC1 and M1 polymers with those reported in the literature.[27,29,31,41−43] The samples were prepared and measured at pH 7 with t_c = 1 h. (g) Schematic representation of the overall adhesion and cohesion mechanism of the PEGtides developed in this study. (h) Chemical structures of the representative polymers. Each experiment was conducted independently at least 3 times, and the average values are reported here with the standard deviations as errors.

The W_{ad} values for the different PEGtides are summarized in Figure 2f. In all cases, the strongest adhesion between PEGtide films, regardless of the measurement conditions, was observed for the AC1 sample, which contained 25% catechol moiety. Interestingly, this catechol ratio is similar to that of DOPA (*ca.* 27%) in natural *mfp*-5, suggesting that the catechol content is a key parameter for enhancing the adhesion. However, a comprehensive understanding of the superior wet adhesion of AC1 in comparison to the other samples with different catechol fractions requires an in-depth evaluation of the underlying molecular characteristics. Thus, the various intermolecular interactions that are primarily responsible for the wet adhesive property of the PEGtides were first identified through MD simulations (see computational details in the Supporting Information, and the modeling system and overall procedure of the MD simulation are shown in Figure S15). Four main interactions were identified: (i) cation−π interactions between catechol and amine;[24,39] (ii) Ar−Ar interactions between catechol and catechol;[11] (iii) various H-bonding interactions among catechols,[40] amines, and ethers; and (iv) other electrostatic and van der Waals interactions (denoted as "others" herein) (Figure 3a).

Consistent with the SFA experimental data, the MD simulation results show the strongest adhesion for the AC1 polymer with a catechol content of 25% at pH 7 (Figure 3b−e and Tables S1−S8). Interestingly, among the four types of

https://doi.org/10.1021/jacs.1c11737
J. Am. Chem. Soc. 2022, 144, 6261−6269

adhesive interactions, H-bonding accounts for most of the total interaction energy (68.9−83.4%) regardless of the catechol content and pH conditions (Figure 3b,c). In all the samples, the magnitude of the H-bonding interactions remained similar between pH 3 and 7, whereas the rest of the three types of interactions (cation−π, Ar−Ar, and other interactions) were the strongest for AC1 in all cases. For the cation−π interactions, the interaction strength increased with the catechol content from AC0 to AC1 and then decreased at higher catechol contents from AC1 to AC3. This synergistic effect originates from the trade-off between phenyl and protonated amine upon increasing the catechol content because both moieties are required to form cation−π interactions. Meanwhile, the Ar−Ar interactions only exhibited a marginal correlation with the catechol content in the sample, and their contribution to the total interaction energy was insignificant (*i.e.*, less than 3%). The other types of interactions were also the strongest in AC1, providing additional interactions for enhanced surface adhesion.

According to numerous previous studies, the cation−π interactions between DOPA and lysine are the primarily responsible for their enhanced wet adhesion. In contrast, our results revealed that the adhesion force in our PEGtide system principally originated from H-bonding. Thus, we further analyzed the contribution of H-bonding to the overall adhesive energy according to 12 types of H-bonding acceptor−donor pairs (Figures 3d−f and S16 and Table S9). Specifically, the type and overall strength of the H-bonding significantly varied depending on the catechol contents and pH conditions. AC1 displayed 6 and 10 different types of H-bonding at pH 3 and 7, respectively (Figure 3d,e). To elucidate the effects of functional groups on the H-bonding, the contributions of functional moieties such as the polyether backbone and side chains, catechol, and amine groups, and amine/ammonium groups were classified in detail (Figures S17−S19). The polyether backbone and side chains contributed significantly to the overall H-bonding, particularly as H-bonding acceptors with other functional groups, such as backbone O−NH_2, backbone O−NH_3^+, backbone O−OH, side O−NH_2, side O−NH_3^+, and side O−OH (Figure S17). The contribution of these polymeric ethers is reduced at higher catechol content and pH, owing to the enhanced participation of other functional groups between the catechol and amine groups.

The other functional moieties cannot be explained solely based on the H-bonding. Thus, we analyzed their contribution to the overall interaction energy (*i.e.*, the sum of all four types of intermolecular interactions) (Figures S20−S22). Because the relative fractions of the catechol and amine groups were inversely proportional to each other; the contribution to the overall interaction energy did not change considerably among the different PEGtides. However, contributions of the catechol−amine interactions (*e.g.*, cation−π, NH_2−OH, OH−NH_2, and OH−NH_3^+) and other electrostatic and van der Waals interactions were found to be the largest for AC1 (Figure S20).

At pH 3, most amine groups in the PEGtides were protonated and acted as cation sources for the cation−π and H-bonding donors. In contrast, amine groups in PEGtides were partially deprotonated at pH 7, thereby increasing the amine-related interactions, while diminishing the contribution of ammonium-related interactions (Figure S21). It is also worth noting that H-bonding from ether oxygen in the side chain contributes more toward the overall interaction than that from the backbone ethers (Figure S22).

In parallel, the adhesion energy between a PEGtide film and a mica surface was evaluated using SFA and MD simulations (Figure S23 and Tables S10−S17). The asymmetric adhesion energy generally follows a trend similar to that observed in symmetric adhesion, with a maximum value in the AC1 sample. Detailed information on the asymmetric adhesion is provided in the Supporting Information.

Encouraged by the previous results, the wet-adhesive properties of AC1, comprising the highest W_{ad} among all the synthesized PEGtides, were further investigated with respect to the preparation pH and molecular weight (M_n = 4−17 kDa). To analyze the effect of preparation and measurement pH conditions, AC1 was deposited on a mica surface at pH 3 and 7 and subsequently measured at pH 3 and 7 (Figure 4a,b). From the results, AC1 prepared at pH 7 showed considerably stronger adhesion (W_{ad} = 52.52 mJ/m^2, measured at pH = 7 and t_c = 1 h) compared to that prepared at pH 3 (W_{ad} = 42.08 mJ/m^2, measured at pH = 7 and t_c = 1 h) (Figure 4b). The stronger adhesion observed at pH 7 can be attributed to the enhanced adsorption of polymers on the mica surface owing to the pK_a of muscovite mica (~2.94).[44]

The adhesion energy of a polymer can be affected by its molecular weight, as the molecular weight can affect the number of binding sites, coating density, entanglements, and rate of molecular rearrangement upon contact. To clarify this aspect, we synthesized AC1 polymers with higher molecular weights and the same ratio between catechol and amine (approximately 25% of catechol), namely, $AC1_{9K}$ and $AC1_{17K}$ (Figures S24−S26 and Table S18). SFA measurement revealed that the W_{ad} values of these polymers are similar to or slightly lower than that of $AC1_{4K}$, demonstrating that the molecular weight is not a critical factor for determining W_{ad} (Figure 4c). Furthermore, the lap shear test results were in good agreement with those of the SFA measurements. The lap shear tests revealed that the molecular-level surface interaction could be readily translated to macroscopic surface adhesion. Specifically, all the specimens displayed cohesive failure, and the measured lap shear stresses were similar between $AC1_{4K}$ and $AC1_{9K}$. However, a low lap shear stress was observed for $AC1_{17K}$, possibly because of the low coating density of this polymer.

As mentioned earlier, the polymeric backbone is crucial for determining polymer properties, such as chain flexibility, molecular mobility, solubility, and molecular interactions. To investigate the effect of the backbone on the adhesion properties, a control polymer with a poly(methyl methacrylate) backbone with a similar DP and catechol content to those of AC1 was designed and synthesized by using identical functional-group-bearing monomers to yield the M1 polymer (Figures S27−S29 and Table S18).

Following the same protocols using SFA, the adhesion energy of M1 was determined to be relatively lower than that of AC1, although the interaction force of M1 was similar between them under the same pH and t_c (Figure 4d,e). Interestingly, the W_{ad} of M1 significantly changed with increasing t_c, while that of AC1 was only marginally affected, suggesting that a more flexible chain facilitates molecular rearrangement (Figure 4e). MD simulation confirmed that AC1 exhibited a faster rate of decrease in the end-to-end distance than M1, indicating better flexibility of the former (Figure S30). Thus, the polyether system proposed in this study has significant advantages over polymers with all-carbon

https://doi.org/10.1021/jacs.1c11737
J. Am. Chem. Soc. 2022, 144, 6261−6269

backbones, such as attaining maximum adhesion much more quickly in aqueous media. Additionally, the relatively lower W_{ad} of M1 could be attributed to the absence of oxygen atoms as H-bonding acceptors in the polymer backbone. However, MD simulation revealed that the absence of oxygen atoms is compensated by H-bonding from the ester and carbonyl groups. Meanwhile, contributions from the side chains, such as the synergistic catechol−amine interaction, were found to be significant in both AC1 and M1. In AC1, an additional contribution from the dynamic H-bonding constructed from the functional groups synergistically increased the other electrostatic and van der Waals interactions, leading to a higher overall interaction energy. This result agrees well with that obtained from the SFA experiments (Figures S31−S33 and Tables S19−S21). Interestingly, it was observed that the natural peptide analogue with identical composition of DOPA and lysine displayed a considerably lower interaction energy than AC1 PEGtide, attributing to a lower degree of multimodal H-bonding (Figures S34 and S35 and Tables S22 and S23).

Finally, we compared the adhesion energy from this study to those of similar mussel-mimetic systems including small molecules,[41] peptides,[42] peptoids,[31] proteins,[27] and polymers[29,43] without chemical crosslinking (Figure 4f,h; Table S22). While the experimental conditions vary among literature studies, it is still remarkable to note that AC1 exhibited outstanding underwater adhesion compared to other systems, demonstrating the highly interactive H-bonding along with the catechol−amine synergy in the proposed PEGtide system (Figure 4g).

CONCLUSIONS

In summary, we presented the design and synthesis of PEGtides, copolyethers comprising two functional epoxide monomers that mimic key amino acid residues, such as DOPA and lysine found in natural *mfp*. A series of PEGtides containing different fractions of catechol and different molecular weights. A series of PEGtides containing different fractions of catechol and molecular weights were prepared *via* anionic ring-opening polymerization followed by subsequent deprotection. The surface adhesive properties of these PEGtides were analyzed using an SFA. A PEGtide with the optimum ratio between the catechol and amine in synergistic interactions displayed the highest adhesion energy of 52.52 mJ/m^2. Furthermore, MD simulations were performed to elucidate the contributions of the diverse intermolecular interactions in PEGtides, particularly to assess the effects of the interplay among catechol and amine, and polyether backbone on the highly adhesive properties of PEGtides. This approach will aid in the design of peptidomimetic polymers with reduced complexity within the framework of a polyether backbone.

ASSOCIATED CONTENT

Supporting Information

The Supporting Information is available free of charge at https://pubs.acs.org/doi/10.1021/jacs.1c11737.

Detailed experimental procedures, detailed ^1H and ^{13}C NMR spectra of the monomer; ^1H NMR spectra, GPC data, and polymerization kinetics of PEGtides; MD simulation model, detailed H-bonding distance calculation of PEGtides, calculated interaction energies, chain flexibility simulation, detailed interaction energy calculation of M1, and additional MD simulation data (PDF)

AUTHOR INFORMATION

Corresponding Authors

Sang Kyu Kwak − *School of Energy and Chemical Engineering, Ulsan National Institute of Science and Technology (UNIST), Ulsan 44919, Republic of Korea;* orcid.org/0000-0002-0332-1534; Email: skkwak@unist.ac.kr

Dong Woog Lee − *School of Energy and Chemical Engineering, Ulsan National Institute of Science and Technology (UNIST), Ulsan 44919, Republic of Korea;* orcid.org/0000-0002-1572-9270; Email: dongwoog.lee@unist.ac.kr

Byeong-Su Kim − *Department of Chemistry, Yonsei University, Seoul 03722, Republic of Korea;* orcid.org/0000-0002-6419-3054; Email: bskim19@yonsei.ac.kr

Authors

Minseong Kim − *Department of Chemistry, Yonsei University, Seoul 03722, Republic of Korea; Department of Chemistry, Ulsan National Institute of Science and Technology (UNIST), Ulsan 44919, Republic of Korea;* orcid.org/0000-0002-2612-922X

Jinwoo Park − *School of Energy and Chemical Engineering, Ulsan National Institute of Science and Technology (UNIST), Ulsan 44919, Republic of Korea;* orcid.org/0000-0003-2921-2923

Kyung Min Lee − *School of Energy and Chemical Engineering, Ulsan National Institute of Science and Technology (UNIST), Ulsan 44919, Republic of Korea*

Eeseul Shin − *Department of Chemistry, Yonsei University, Seoul 03722, Republic of Korea*

Suebin Park − *Department of Chemistry, Yonsei University, Seoul 03722, Republic of Korea;* orcid.org/0000-0002-4677-076X

Joonhee Lee − *Department of Chemistry, Yonsei University, Seoul 03722, Republic of Korea*

Chanoong Lim − *School of Energy and Chemical Engineering, Ulsan National Institute of Science and Technology (UNIST), Ulsan 44919, Republic of Korea;* orcid.org/0000-0001-6903-0855

Complete contact information is available at: https://pubs.acs.org/10.1021/jacs.1c11737

Author Contributions

‖M.K., J.P., and K.M.L. contributed equally to this work.

Notes

The authors declare no competing financial interest.

ACKNOWLEDGMENTS

This work was supported by the Samsung Research Funding & Incubation Center of Samsung Electronics under project number SRFC-MA1602-07. This work was also partially supported by the National Research Foundation of Korea (NRF-2021R1A2C3004978).

REFERENCES

(1) Levin, A.; Hakala, T. A.; Schnaider, L.; Bernardes, G. J. L.; Gazit, E.; Knowles, T. P. J. Biomimetic Peptide Self-Assembly for Functional Materials. *Nat. Rev. Chem.* **2020**, *4*, 615−634.

(2) Ergene, C.; Yasuhara, K.; Palermo, E. F. Biomimetic Antimicrobial Polymers: Recent Advances in Molecular Design. *Polym. Chem.* **2018**, *9*, 2407−2427.
(3) Sedó, J.; Saiz-Poseu, J.; Busqué, F.; Ruiz-Molina, D. Catechol-Based Biomimetic Functional Materials. *Adv. Mater.* **2013**, *25*, 653−701.
(4) Méndez-Samperio, P. Peptidomimetics as a New Generation of Antimicrobial Agents: Current Progress. *Infect. Drug Resist.* **2014**, *7*, 229−237.
(5) Chongsiriwatana, N. P.; Patch, J. A.; Czyzewski, A. M.; Dohm, M. T.; Ivankin, A.; Gidalevitz, D.; Zuckermann, R. N.; Barron, A. E. Peptoids That Mimic the Structure, Function, and Mechanism of Helical Antimicrobial Peptides. *Proc. Natl. Acad. Sci. U.S.A.* **2008**, *105*, 2794−2799.
(6) Takahashi, H.; Caputo, G. A.; Vemparala, S.; Kuroda, K. Synthetic Random Copolymers as a Molecular Platform to Mimic Host-Defense Antimicrobial Peptides. *Bioconjugate Chem.* **2017**, *28*, 1340−1350.
(7) Chongsiriwatana, N. P.; Miller, T. M.; Wetzler, M.; Vakulenko, S.; Karlsson, A. J.; Palecek, S. P.; Mobashery, S.; Barron, A. E. Short Alkylated Peptoid Mimics of Antimicrobial Lipopeptides. *Antimicrob. Agents Chemother.* **2011**, *55*, 417−420.
(8) Kim, M.; Mun, W.; Jung, W. H.; Lee, J.; Cho, G.; Kwon, J.; Ahn, D. J.; Mitchell, R. J.; Kim, B.-S. Antimicrobial PEGtides: A Modular Poly(Ethylene Glycol)-Based Peptidomimetic Approach to Combat Bacteria. *ACS Nano* **2021**, *15*, 9143−9153.
(9) Engler, A. C.; Shukla, A.; Puranam, S.; Buss, H. G.; Jreige, N.; Hammond, P. T. Effects of Side Group Functionality and Molecular Weight on the Activity of Synthetic Antimicrobial Polypeptides. *Biomacromolecules* **2011**, *12*, 1666−1674.
(10) Ahn, B. K. Perspectives on Mussel-Inspired Wet Adhesion. *J. Am. Chem. Soc.* **2017**, *139*, 10166−10171.
(11) Waiter, J. H. Reverse Engineering of Bioadhesion in Marine Mussels. *Ann. N.Y. Acad. Sci.* **1999**, *875*, 301−309.
(12) Waite, J. H.; Qin, X. Polyphosphoprotein from the Adhesive Pads of *Mytilus Edulis*. *Biochemistry* **2001**, *40*, 2887−2893.
(13) Yu, M.; Hwang, J.; Deming, T. J. Role of 1-3,4-Dihydroxyphenylalanine in Mussel Adhesive Proteins. *J. Am. Chem. Soc.* **1999**, *121*, 5825−5826.
(14) Lin, Q.; Gourdon, D.; Sun, C.; Holten-Andersen, N.; Anderson, T. H.; Waite, J. H.; Israelachvili, J. N. Adhesion Mechanisms of the Mussel Foot Proteins Mfp-1 and Mfp-3. *Proc. Natl. Acad. Sci. U.S.A.* **2007**, *104*, 3782−3786.
(15) Petrone, L.; Kumar, A.; Sutanto, C. N.; Patil, N. J.; Kannan, S.; Palaniappan, A.; Amini, S.; Zappone, B.; Verma, C.; Miserez, A. Mussel Adhesion Is Dictated by Time-Regulated Secretion and Molecular Conformation of Mussel Adhesive Proteins. *Nat. Commun.* **2015**, *6*, 8737.
(16) Danner, E. W.; Kan, Y.; Hammer, M. U.; Israelachvili, J. N.; Waite, J. H. Adhesion of Mussel Foot Protein Mefp-5 to Mica: An Underwater Superglue. *Biochemistry* **2012**, *51*, 6511−6518.
(17) Lu, Q.; Danner, E.; Waite, J. H.; Israelachvili, J. N.; Zeng, H.; Hwang, D. S. Adhesion of Mussel Foot Proteins to Different Substrate Surfaces. *J. R. Soc., Interface* **2013**, *10*, 20120759.
(18) Lee, H.; Scherer, N. F.; Messersmith, P. B. Single-Molecule Mechanics of Mussel Adhesion. *Proc. Natl. Acad. Sci. U.S.A.* **2006**, *103*, 12999−13003.
(19) Yu, J.; Wei, W.; Danner, E.; Israelachvili, J. N.; Waite, J. H. Effects of Interfacial Redox in Mussel Adhesive Protein Films on Mica. *Adv. Mater.* **2011**, *23*, 2362−2366.
(20) Ahn, B. K.; Das, S.; Linstadt, R.; Kaufman, Y.; Martinez-Rodriguez, N. R.; Mirshafian, R.; Kesselman, E.; Talmon, Y.; Lipshutz, B. H.; Israelachvili, J. N.; Waite, J. H. High-Performance Mussel-Inspired Adhesives of Reduced Complexity. *Nat. Commun.* **2015**, *6*, 8663.
(21) Wei, Q.; Achazi, K.; Liebe, H.; Schulz, A.; Noeske, P.-L. M.; Grunwald, I.; Haag, R. Mussel-Inspired Dendritic Polymers as Universal Multifunctional Coatings. *Angew. Chem., Int. Ed.* **2014**, *53*, 11650−11655.
(22) Wei, W.; Yu, J.; Gebbie, M. A.; Tan, Y.; Martinez Rodriguez, N. R.; Israelachvili, J. N.; Waite, J. H. Bridging Adhesion of Mussel-Inspired Peptides: Role of Charge, Chain Length, and Surface Type. *Langmuir* **2015**, *31*, 1105−1112.
(23) Gallivan, J. P.; Dougherty, D. A. A Computational Study of Cation-π Interactions vs Salt Bridges in Aqueous Media: Implications for Protein Engineering. *J. Am. Chem. Soc.* **2000**, *122*, 870−874.
(24) Gebbie, M. A.; Wei, W.; Schrader, A. M.; Cristiani, T. R.; Dobbs, H. A.; Idso, M.; Chmelka, B. F.; Waite, J. H.; Israelachvili, J. N. Tuning Underwater Adhesion with Cation-π Interactions. *Nat. Chem.* **2017**, *9*, 473−479.
(25) Podsiadlo, P.; Liu, Z.; Paterson, D.; Messersmith, P. B.; Kotov, N. A. Fusion of Seashell Nacre and Marine Bioadhesive Analogs: High-Strength Nanocomposite by Layer-by-Layer Assembly of Clay and L-3,4- Dihydroxyphenylalanine Polymer. *Adv. Mater.* **2007**, *19*, 949−955.
(26) Liu, B.; Burdine, L.; Kodadek, T. Chemistry of Periodate-Mediated Cross-Linking of 3,4-Dihydroxylphenylalanine-Containing Molecules to Proteins. *J. Am. Chem. Soc.* **2006**, *128*, 15228−15235.
(27) Seo, S.; Das, S.; Zalicki, P. J.; Mirshafian, R.; Eisenbach, C. D.; Israelachvili, J. N.; Waite, J. H.; Ahn, B. K. Microphase Behavior and Enhanced Wet-Cohesion of Synthetic Copolyampholytes Inspired by a Mussel Foot Protein. *J. Am. Chem. Soc.* **2015**, *137*, 9214−9217.
(28) Rapp, M. V.; Maier, G. P.; Dobbs, H. A.; Higdon, N. J.; Waite, J. H.; Butler, A.; Israelachvili, J. N. Defining the Catechol-Cation Synergy for Enhanced Wet Adhesion to Mineral Surfaces. *J. Am. Chem. Soc.* **2016**, *138*, 9013−9016.
(29) Maier, G. P.; Rapp, M. V.; Waite, J. H.; Israelachvili, J. N.; Butler, A. Adaptive Synergy between Catechol and Lysine Promotes Wet Adhesion by Surface Salt Displacement. *Science* **2015**, *349*, 628−632.
(30) Tiu, B. D. B.; Delparastan, P.; Ney, M. R.; Gerst, M.; Messersmith, P. B. Cooperativity of Catechols and Amines in High-Performance Dry/Wet Adhesives. *Angew. Chem., Int. Ed.* **2020**, *59*, 16616−16624.
(31) Wonderly, W. R.; Cristiani, T. R.; Cunha, K. C.; Degen, G. D.; Shea, J.-E.; Waite, J. H. Dueling Backbones: Comparing Peptoid and Peptide Analogues of a Mussel Adhesive Protein. *Macromolecules* **2020**, *53*, 6767−6779.
(32) Lee, J.; Han, S.; Kim, M.; Kim, B.-S. Anionic Polymerization of Azidoalkyl Glycidyl Ethers and Post-Polymerization Modification. *Macromolecules* **2020**, *53*, 355−366.
(33) Niederer, K.; Schüll, C.; Leibig, D.; Johann, T.; Frey, H. Catechol Acetonide Glycidyl Ether (CAGE): A Functional Epoxide Monomer for Linear and Hyperbranched Multi-Catechol Functional Polyether Architectures. *Macromolecules* **2016**, *49*, 1655−1665.
(34) Beckingham, B. S.; Sanoja, G. E.; Lynd, N. A. Simple and Accurate Determination of Reactivity Ratios Using a Nonterminal Model of Chain Copolymerization. *Macromolecules* **2015**, *48*, 6922−6930.
(35) Johnson, K. L.; Kevin, K.; Roberts, A. D. Surface Energy and the Contact of Elastic Solids. *Proc. R. Soc. London, Ser. A* **1971**, *324*, 301−313.
(36) Lee, D. W.; Lim, C.; Israelachvili, J. N.; Hwang, D. S. Strong Adhesion and Cohesion of Chitosan in Aqueous Solutions. *Langmuir* **2013**, *29*, 14222−14229.
(37) Lim, C.; Lee, D. W.; Israelachvili, J. N.; Jho, Y.; Hwang, D. S. Contact Time- and pH-Dependent Adhesion and Cohesion of Low Molecular Weight Chitosan Coated Surfaces. *Carbohydr. Polym.* **2015**, *117*, 887−894.
(38) Lee, J. H.; Lee, D. W. Contact-Induced Molecular Rearrangement of Acrylic Acid-Incorporated Pressure Sensitive Adhesives. *Appl. Surf. Sci.* **2020**, *500*, 144246.
(39) Lyu, Q.; Hsueh, N.; Chai, C. L. L. The Chemistry of Bioinspired Catechol(Amine)-Based Coatings. *ACS Biomater. Sci. Eng.* **2019**, *5*, 2708−2724.
(40) Ahn, B. K.; Lee, D. W.; Israelachvili, J. N.; Waite, J. H. Surface-Initiated Self-Healing of Polymers in Aqueous Media. *Nat. Mater.* **2014**, *13*, 867−872.

https://doi.org/10.1021/jacs.1c11737
J. Am. Chem. Soc. 2022, 144, 6261−6269

(41) Degen, G. D.; Stow, P. R.; Lewis, R. B.; Andresen Eguiluz, R. C.; Valois, E.; Kristiansen, K.; Butler, A.; Israelachvili, J. N. Impact of Molecular Architecture and Adsorption Density on Adhesion of Mussel-Inspired Surface Primers with Catechol-Cation Synergy. *J. Am. Chem. Soc.* **2019**, *141*, 18673−18681.
(42) Zhang, C.; Xiang, L.; Zhang, J.; Gong, L.; Han, L.; Xu, Z.-K.; Zeng, H. Tough and Alkaline-Resistant Mussel-Inspired Wet Adhesion with Surface Salt Displacement via Polydopamine/Amine Synergy. *Langmuir* **2019**, *35*, 5257−5263.
(43) Lim, C.; Huang, J.; Kim, S.; Lee, H.; Zeng, H.; Hwang, D. S. Nanomechanics of Poly(Catecholamine) Coatings in Aqueous Solutions. *Angew. Chem., Int. Ed.* **2016**, *55*, 3342−3346.
(44) Maslova, M. V.; Gerasimova, L. G.; Forsling, W. Surface Properties of Cleaved Mica. *Colloid J.* **2004**, *66*, 322−328.

https://doi.org/10.1021/jacs.1c11737
J. Am. Chem. Soc. 2022, 144, 6261−6269